Magneto-optical Linear Dichroism in Threshold Photoemission Electron Microscopy of Polycrystalline Fe Films

G. K. L. Marx, H. J. Elmers, and G. Schönhense
Johannes Gutenberg-Universität Mainz, Staudingerweg 7, D-55099 Mainz, Germany
(Received 14 July 1999; revised manuscript received 31 January 2000)

Magnetic linear dichroism in threshold photoemission has been exploited to obtain magnetic contrast in a photoemission electron microscope using a mercury arc lamp. The dichroism at threshold can be described similar to the magneto-optical Kerr effect in the region of visible light. The asymmetry of electron intensity observed for a 100 nm polycrystalline Fe film on silicon is $A = (0.37 \pm 0.05)\%$. The asymmetry occurs for the geometry of the transverse Kerr effect. For unpolarized light the asymmetry was about half the value observed for linearly polarized light. Threshold photoemission microscopy has a large potential for high resolution magnetic domain imaging with fast data acquisition.

PACS numbers: 75.70.Kw, 07.78.+s

Threshold photoemission is the key experiment for the concept of the quantized nature of light [1]. Since then, photoemission has been preferentially described as a single particle excitation process. At higher photon energies this picture is an adequate model. The photoabsorption step can be described as a single electron excitation process which can quite easily be understood using Fermi's golden rule. For the case of magnetic thin films and surfaces, respective spectroscopic information on directly emitted photoelectrons revealed the presence of a magnetic circular [2,3] and linear [4] dichroic effect close to the Fermi energy. This magnetic dichroism in photoemission greatly increased the knowledge about the electronic structure of ferromagnets [5]. Moreover, using the high intensity of synchrotron sources, both linear [6] and circular dichroism [7–9] effects have been used to image magnetic domains with high resolution.

In the case of threshold photoemission the excitation process is more complex because usually no final states are available in the real part of the band structure [5]. Moreover, the high density of initial states inhibits a description as a single electron process [10,11]. The process is governed by collective electron excitations. For the case of photon reflection in the energy regime of visible light, the reflection and absorption process has been successfully described with metal optics using complex refraction constants. The magnetic dichroism effect in light reflection is known as the magneto-optical Kerr effect [12]. A simple picture describes this effect as dipole radiation from excited collective electron oscillations, where the oscillation axis is rotated as a consequence of the Lorentz force acting inside the ferromagnetic metal [13]. Of course, in order to gain quantitative information detailed theoretical calculations involving the band structure are necessary [14]. However, the result of the calculations can be described by a complex rotation angle, thus greatly simplifying the description for different geometries [14].

It is the purpose of this Letter to show that a magnetic dichroic asymmetry exists for photoelectrons excited at threshold, too. The measured value for the asymmetry strongly suggests the same simple model used for the case of the magneto-optical Kerr effect. Using photoemission electron microscopy (PEEM), the dichroism in photoemission can be used to image magnetic domains *in situ* in UHV with a lateral resolution superior to *in situ* Kerr microscopy [15,16] and with a higher data acquisition frequency per pixel than high resolution scanning approaches like scanning electron microscopy with polarization analysis [17–19] or spin-polarized tunneling microscopy [20], while spin-polarized low energy electron microscopy [21] could not be applied to polycrystalline films, yet, and Lorentz microscopy being based on the transmission of a high energy electron beam lacks surface sensitivity [22].

The experiment used a UHV high resolution photoemission microscope featuring a triode objective lens system, selectable contrast apertures, and a two-stage projective. The image is displayed on a phosphor screen and subsequently captured by a slow scan charge-coupled device camera. Numerical simulations of the electron trajectories for typical experimental conditions indicate that only electrons with starting angles less than 10° with respect to the surface normal contribute to the image. A Hg high pressure arc lamp (100 W) delivering a spectrum with photon energies $\hbar\omega \leq 5.0$ eV served as the illumination source. The light beam was focused and sent through a linear polarizer (Glan-Thompson prism), before it impinged onto the sample surface at grazing incidence ($\alpha_1 = 75°$). The solid angle of sample illumination was $\pm 5°$. By rotating the prism the linear polarization could be changed continuously between *s*- and *p*-polarized states, however, the magnetic contrast was observed only for *p*-polarized light, i.e., when the electric vector is in the plane of incidence.

The polycrystalline iron film with a thickness of 100 nm has been deposited by means of UHV evaporation (base pressure 4×10^{-10} mbar) on a silicon wafer with a native oxide layer. The evaporation rate (typically 1.6 nm per minute at $p = 1 \times 10^{-9}$ mbar) was controlled by a quartz

 0031-9007/00/84(25)/5888(4)$15.00

thickness monitor. The sample holder allowed *in situ* application of an external magnetic field. The work function of the films (4.5 eV) limits the energy width of the photoelectron distribution to about $\Delta E \leq 0.5$ eV.

In order to extract the magnetic contrast from the images, it is advantageous to subtract a "reference image" (taken with a fully magnetized sample), a technique which is known from Kerr microscopy [12]. In the resulting difference image, other contrast contributions such as work function contrast, topographical contrast, impurities, etc. are largely eliminated. Figure 1 shows an example of the resulting magnetic contrast. In this case a series of images was taken during a magnetization procedure. After demagnetization with an ac field (50 Hz) the film has been exposed to a field of 2.53 mT perpendicular to the plane of incidence. Then, the left image has been taken in zero field. Next, a field of 2.61 mT was applied, yielding the second image in zero field. The last image taken after a field of 4 mT was applied was then subtracted from the previous images. In this way, the stepwise growth of the bright domains (magnetization pointing to the right) became visible. The remaining features originate from topographic contrast, which is greatly enhanced due to a small shift between original and reference image. The series of images with "moving" domains proves the existence of a true magnetic asymmetry in photoemission. The configuration of incident light and magnetization direction being perpendicular to each other is known as the transverse geometry. For reflected light an asymmetry originates from the transversal magneto-optical Kerr effect [12]. For photoemission spectroscopy the usual term for the asymmetry observed in our experiment is linear magnetic dichroism (LMD) [6]. The asymmetry extracted from the areas of opposite magnetization is

$$A_{\mathrm{LMD}} = \frac{I(M^+) - I(M^-)}{I(M^+) + I(M^-)} = (0.37 \pm 0.05)\% . \quad (1)$$

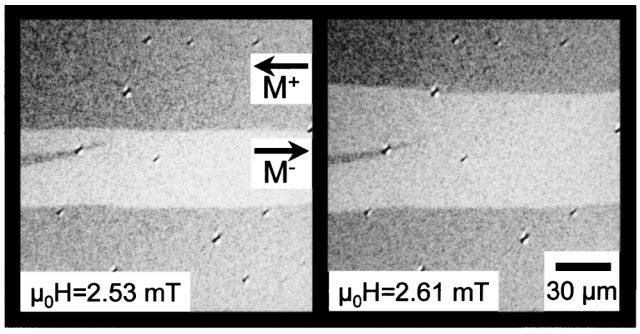

FIG. 1. Magnetic domain patterns of a polycrystalline Fe film. In order to eliminate contrast contributions other than magnetic, a "reference image" taken with the sample in a single domain state has been subtracted. A stepwise increased external field as indicated in the images was applied prior to exposure at zero field. The "black" domains become smaller as the field increases finally vanishing at the coercive field of 4 mT.

No asymmetry was observed for magnetization direction in the plane of incidence, i.e., in the longitudinal geometry.

For the investigation of lateral resolution we present in Fig. 2a a highly magnified image showing only two magnetic domains with a horizontal domain wall. The image was taken with unpolarized light in order to avoid the small aperture (10 mm) of our Glan-Thompson polarizer and thus increasing the light intensity roughly by a factor of 6. Since unpolarized light consists of a 50% contribution of p polarization, an unpolarized photon beam can be used for magnetic imaging, too. We observed an asymmetry of $A_{\mathrm{unpol}} = (0.18 \pm 0.05)\%$, which is about half the value obtained for linearly polarized light. This result is expected when metal optics are neglected. Since the polarizing effect of a metal surface increases p polarization inside the metal one would expect an asymmetry between A_{LMD} and $A_{\mathrm{LMD}}/2$ for unpolarized light. Figure 2a represents a field of view of $20 \times 8.8\ \mu\mathrm{m}^2$. The total exposure time was 360 s per image. A line scan averaged over 280 lines across the magnetic domain wall is shown in Fig. 2b. Using the classical definition of the domain wall width based on the slope in the center of the transition the width results to 0.4 μm. This value represents an upper value for the lateral resolution.

The width of the transition between the two domains is the convolution of the domain wall width and the effective lateral resolution of the instrument. The intrinsic domain wall width of a Bloch wall within an Fe single crystal is 55 nm. However, at the surface of a single crystal an asymmetric Bloch wall broadens the transition to

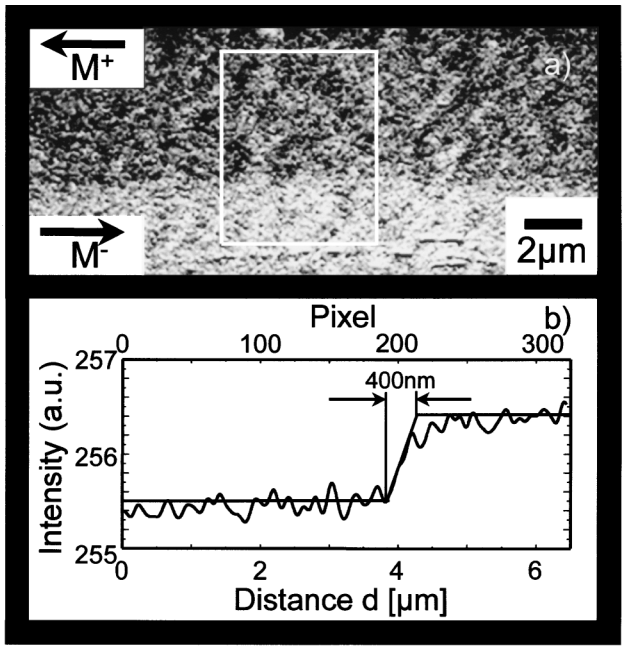

FIG. 2. (a) Highly magnified image of a domain pattern. Only a single domain wall appears in the image. (b) Intensity line scan across the area indicated in (a).

about 150 nm [18]. We expect similar asymmetric Bloch walls in our case because a comparison of wall energies for thin films [12] suggests this wall type is favorable for Fe films thicker than 30 nm. The wall width might be even larger because the films are polycrystalline. Calculations of magnetostatic energy distributions predict that the mean magnetostatic energy of a cubic polycrystal is about 0.20 that of separated single crystalline grains, so that its domain width will be $1/\sqrt{0.20} = 2.2$ times larger [23]. In threshold photoemission only electrons in a narrow window of 0.0–0.5 eV below the Fermi energy can contribute to the image. Thus, an energy filter decreasing the dispersion is obsolete. A lateral resolution of better than 25 nm [24] has been demonstrated for PEEM in threshold photoemission. Therefore, the lateral resolution of the instrument is small compared to the domain wall width. However, the extremely small magnetic contrast in combination with the relatively low UV-light intensity of the mercury arc lamp used in our experiment gives rise to an additional broadening of the apparent wall profile. First, if the domain wall was not a perfectly straight line, the averaging of line scans, necessary to gain signal to noise ratio, would result in a broadening of the profile. Second, a lateral drift of the sample holder during exposure cannot be completely excluded.

In the following we will present a simple theoretical model which can qualitatively explain the observed asymmetries. Threshold photoemission for metals cannot be described by direct interband transitions, because no real final states exist in the region just above the vacuum level [25]. Consequently, threshold photoemission is rather treated using evanescent final states as described by Sass [11]. To first order, the probability P of electron emission from a polycrystalline material is given by the square of the scalar product of the electron momentum $\vec{k}$ and electric vector $\vec{E}$ within the solid [10], $P \propto (\vec{E} \cdot \vec{k})^2$, indicating that the electron intensity is increased for grazing incident light. For magnetic materials $\vec{E}$ should be replaced by the displacement vector $\vec{D} = \underline{\epsilon}\epsilon_0\vec{E}$ with the dielectric tensor $\underline{\epsilon}$ [12] which causes a rotation of $\vec{D}$ due to the nondiagonal components arising from the magnetization. The resulting emission intensity is illustrated schematically in Fig. 3. The intensity actually observed in the experiment is given by the sectional volume of the probability distribution (shaded) with the emission cone around the z axis accepted by the microscope optics. The magnetization vector is perpendicular to the drawing plane and pointing upwards in the top figure. In the top figure, the counterclockwise rotation of the probability distribution results in an enhancement of the sectional volume (dark shaded area) as compared with the situation for a clockwise rotation, i.e., downward magnetization (bottom figure). The intensity of reflected light and the intensity of photoelectrons is enhanced for the same magnetization direction (top figure), i.e., the asymmetries of photoemission A_{LMD} and of reflected light A_K have the same sign.

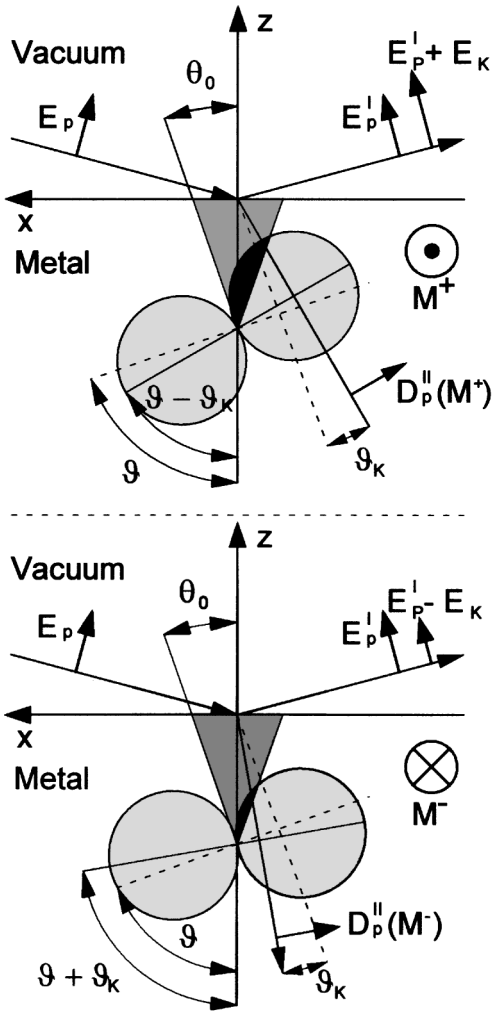

FIG. 3. Schematic illustration of the origin of the magnetic contrast. Because of the Lorentz force inside of the material the displacement vector rotates, which causes the well-known intensity change in the reflected beam, i.e., in the transverse Kerr effect. The intensity of emitted electrons is proportional to the sectional volume (dark shaded area) between the emission cone of electrons accepted from the electron microscope (shaded area) and the probability distribution of electron emission. A rotation of the displacement vector increases (top figure) or decreases (bottom figure) the intensity.

For a quantitative discussion of the model metal optics are essential. Taking into account the emission cone of photoemitted electrons, the probability of electron emission can be written as [10,11]

$$P(\vartheta, \theta_0) \propto \sin^2\theta_0 + \cos^2\vartheta(3\cos^2\theta_0 - 1), \qquad (2)$$

where θ_0 denotes the maximum inner emission angle within the solid with respect to the surface normal. The angle ϑ is defined by the angle between surface normal and the displacement vector inside the solid (see Fig. 3). From the angle of photon incidence $\alpha_1 = 75°$ and the complex refractive index $\tilde{n}_{\mathrm{Fe}} = 1.42 + 2.05i$ (which differs from the value $n_{\mathrm{Fe}} = 1.14 + 1.87i$ of

bulk Fe determined at normal incidence [14]) ϑ can be estimated to be approximately $\vartheta = 47°$ [26]. The emission angle θ of electrons in vacuum is limited by the contrast aperture of the microscope to a value of about $\theta = 10°$. Because of the inner attractive potential inside the metal (13 eV in the case of Fe [27]) the maximum emission angle inside the solid, $\theta_0 = 6.4°$, is even smaller and therefore the influence on the asymmetry is nearly negligible. The magnetization-induced Kerr rotation ϑ_K of the displacement vector inside the material could be estimated from the experimentally determined transverse Kerr asymmetry A_K. Using the Fresnel formalism for the reflection of light from metal surfaces [26] ϑ_K results from the variation of the angle $\alpha_2 = \pi/2 - \vartheta$ between the propagation direction of the light inside the metal and the surface normal (see Fig. 3) which is necessary to obtain the experimentally observed asymmetry of the reflection coefficient:

$$\vartheta_K = \mathrm{Re}\left(\frac{\tilde{n}_{\mathrm{Fe}}^2 \cos\alpha_1 - \sqrt{\tilde{n}_{\mathrm{Fe}}^2 - \sin^2\alpha_1}}{\sin\alpha_1}\right)\frac{A_K}{4}. \quad (3)$$

The experimental value $A_K = 0.0039$ determined for the same incident angle as in the case of photoemission results in $\vartheta_K = 0.11°$.

The asymmetry in photoemission results from the emission probability P as

$$A_{\mathrm{LMD}} = \frac{P(\vartheta - \vartheta_K, \theta_0) - P(\vartheta + \vartheta_K, \theta_0)}{P(\vartheta - \vartheta_K, \theta_0) + P(\vartheta + \vartheta_K, \theta_0)}. \quad (4)$$

Insertion of the numerical values gives an expected asymmetry of $A_{\mathrm{LMD}} = 0.0041$. This estimation is in reasonable quantitative agreement with the measured asymmetry of 0.0037. The agreement suggests that the observed magnetic linear dichroism asymmetry in threshold photoemission is a direct consequence of a Kerr-effect-like rotation of the electric vector inside of a magnetic material. It has the same origin as the transverse Kerr effect being observed under the same experimental conditions in the reflected photon intensity.

In conclusion, magnetic linear dichroism in threshold photoelectron emission has been detected for polycrystalline Fe films. The dichroism asymmetry of 0.37% has been exploited for magnetic domain imaging using a PEEM. The dichroism asymmetry is comparable to the asymmetry observed in the transverse Kerr effect for the same samples. The asymmetry could be quantitatively explained in a simple model treating quasifree electrons. The effect arises due to an interplay between metal optics and Kerr rotation of the displacement vector inside the material. The contrast mechanism arises also for incident unpolarized light. The effect occurs in the geometry of the transverse Kerr effect. Although the first results have been measured for thin Fe films, the phenomenon has the same general physical origin as the magneto-optical Kerr effect. It will thus not be restricted to a specific class of materials. At present, we achieved a lateral resolution of better than 400 nm. It is likely that the practical limit in lateral resolution of 25 nm observed for topographical contrast can be achieved for magnetic contrast, too. Because of its potential for high resolution and the efficient parallel image acquisition, the new method is highly attractive for applications.

Our thanks are due to C. M. Schneider for valuable contributions during the early stages of the work. The experiment has been funded by Materialwissenschaftliches Forschungszentrum Mainz (MWFZ) and Sonderforschungsbereich 262.

[1] A. Einstein, Ann. Phys. (Leipzig) **17**, 132 (1905).
[2] C. M. Schneider *et al.,* J. Phys. Condens. Matter **6**, 1177 (1994).
[3] W. Kuch *et al.,* Phys. Rev. B **53**, 11 621 (1996).
[4] A. Rampe *et al.,* Phys. Rev. B **57**, 14 370 (1998).
[5] F. J. Himpsel, Adv. Phys. **47**, 511 (1998).
[6] F. U. Hillebrecht *et al.,* Phys. Rev. Lett. **75**, 2224 (1995).
[7] J. Stöhr *et al.,* Science **259**, 658 (1993).
[8] G. Lilienkamp *et al.,* in *X-Ray Microscopy and Spectromicroscopy,* edited by J. Thieme, B. Schmahl, D. Rudolf, and E. Umbach (Springer, New York, 1998).
[9] W. Swiech *et al.,* J. Electron Spectrosc. Relat. Phenom. **84**, 171 (1997).
[10] G. P. Mahan, Phys. Rev. B **2**, 4334 (1970).
[11] J. K. Sass, Surf. Sci **51**, 199 (1975).
[12] A. Hubert and R. Schäfer, *Magnetic Domains* (Springer, New York, 1998).
[13] J. L. Erskine and E. A. Stern, Phys. Rev. B **8**, 1239 (1973).
[14] P. M. Oppeneer *et al.,* Phys. Rev. B **45**, 10 924 (1992).
[15] J. Giergiel and J. Kirschner, Rev. Sci. Instrum. **67**, 2937 (1996).
[16] E. Mentz *et al.,* Phys. Rev. B **60**, 7379 (1999).
[17] K. Koike and K. Hayakawa, Jpn. J. Appl. Phys. **23**, L187 (1984).
[18] H. P. Oepen and J. Kirschner, Phys. Rev. Lett. **62**, 819 (1989).
[19] J. Unguris *et al.,* Phys. Rev. Lett. **67**, 140 (1991).
[20] M. Bode *et al.,* Phys. Rev. Lett. **81**, 4256 (1998).
[21] M. S. Altman *et al.,* Mater. Res. Soc. Symp. Proc. **232**, 125 (1990).
[22] J. N. Chapman, J. Phys. D **17**, 623 (1984).
[23] S. Chikazumi, *Physics of Ferromagnetism* (Oxford Science Publishing, New York, 1997).
[24] G. K. L. Marx *et al.,* J. Electron Spectrosc. Relat. Phenom. **84**, 251 (1997).
[25] J. Callaway *et al.,* Phys. Rev. B **16**, 2095 (1977).
[26] M. Born and E. Wolf, *Principles of Optics* (Pergamon Press Ltd., London, 1959).
[27] M. Albrecht *et al.,* Solid State Commun. **78**, 671 (1991).